BMC Medical Genomics

RESEARCH

Open Access

A novel homozygous splicing variant in *FREM1* expands the phenotypic spectrum of BNAR syndrome: functional validation and successful PGT-M

Lulu Yan[1,2,3], Yingwen Liu[1,2,3], Yuxin Zhang[1,2,3], Chunxiao Han[1,2,3], Juan Cao[4], Jinghui Zou[5], Hongjing Luo[4] and Haibo Li[1,2,3*]

Abstract

Background Bifid nose with or without anorectal and renal anomalies (BNAR) is a rare autosomal recessive genetic congenital disorder characterized by bifid nose and renal agenesis, with or without anorectal malformations. Our research identified the genetic factors associated with BNAR in a Chinese pedigree.

Methods Muscle tissue specimens from the fetus and peripheral blood specimens from the parents were collected, and genomic DNA was extracted for whole-exome sequencing. Sanger sequencing was used to verify the emergence of variants in the pedigree. Minigene assays and structural modeling were performed to confirm the influence of intronic variants on mRNA splicing.

Results We identified a homozygous splicing variant, c.3274 + 4 A > G, in the *FREM1* gene in the fetus. Sanger sequencing revealed that the parents were heterozygous. In vitro and *in intro* minigene assays revealed exon 18 skipping, causing a nonframeshift, 62 amino acid deletion in FREM1. Structural predictions indicate the deletion severely disrupts the FREM1 CSPG6 domain, replacing its stable interwoven β-sheet architecture with a single β-sheet and an aberrant α-helix. This profound conformational shift likely abolishes the interaction interfaces required for FRAS1/FREM multiprotein complex assembly, impairing its overall function. Based on these findings, the variant was categorized as likely pathogenic according to the American College of Medical Genetics and Genomics guidelines. Accordingly, after being informed about the hazards of the pathogenic variant, the couple selected preimplantation genetic tests for monogenic disorders (PGT-M) and had a healthy baby.

Conclusion This study presents a Chinese fetus with *FREM1*-related pathology. Moreover, this study extends the phenotypic spectrum of BNAR, while laying a foundation for PGT-M.

Keywords Bifid nose with or without anorectal and renal anomalies, *FREM1* gene, Splicing Variant, Whole exome sequencing, Minigene assay

*Correspondence:
Haibo Li
lihaibo-775@163.com

Full list of author information is available at the end of the article

Introduction

Bifid nose with or without anorectal and renal anomalies (BNAR, MIM 608980) syndrome is a rare congenital anomaly characterized by a bifid nose and renal agenesis in the presence or absence of anorectal malformations and without intellectual disability [1, 2]. A bifid nose is a congenital malformation caused by paired nasal processes that fail to fuse to a single midline organ in early gestation [2]. BNAR can be triggered by homozygous or complex heterozygous variants in the *FREM1* gene, which encodes a basement membrane protein that may play a role in craniofacial and renal progress [1, 2].

FREM1 encodes FRAS1-related extracellular matrix (ECM) protein 1, which belongs to the FRAS1/FREM family of ECM proteins, and is localized to the sublamina densa of epithelial basement membranes during embryonic development in mammals [3]. FREM1 forms a ternary complex with other ECM proteins, such as FRAS1 and FREM2 [4]. This ternary complex is important for maintaining epithelial-mesenchymal cohesion during embryonic development in mammals [3]. *FREM1* pathogenic variants in humans are predicted to disrupt interactions with proteins in this complex, without reducing the expression levels of FRAS1 and FREM2 [5]. Disruption or loss of the ternary complex decreases epithelial-mesenchymal adhesion during development, and the subsequent generation of characteristic clinical manifestations are related to Fraser syndrome and *FREM1* autosomal recessive conditions [6]. Recently, only 13 cases of BNAR syndrome from five unrelated families have been reported to have mutations in *FREM1* [1, 2, 7, 8]. However, genotype-phenotype relationships may not exist in view of the rarity of the condition and the limited number of described variants.

This study describes a Chinese fetus with BNAR that exhibited a typical clinical phenotype associated with BNAR, in addition to a clinical symptom that has not been previously reported. The variant was functionally characterized using a minigene assay, which revealed variant-induced abnormal splicing events. Our findings clarify the pathogenicity of the splice variant, expand the clinical spectrum of BNAR-related phenotypes, and provide evidence for subsequent pregnancies in patients.

Materials and methods

Clinical examinations

The Chinese family member was recruited the Affiliated Women and Children's Hospital of Ningbo University, Ningbo, China. Figure 1A shows the family pedigree. The proband was a fetus suspected of suffering from intracranial hemorrhage, fetal left renal hydronephrosis, and upper ureteral obstruction based on a prenatal ultrasound at 32 weeks of gestation (Fig. 1B, C). Left hydronephrosis was confirmed using magnetic resonance imaging (MRI) at 32 weeks and 2 days of pregnancy, and hydrocephalus, intracerebral hemorrhage into the left ventricle, left subdural hemorrhage, and subarachnoid hemorrhage were observed (Fig. 1D, F). The parents were non-consanguineous. This was their first pregnancy and there was no relevant family history. After being completely informed about the fetal prognosis and undergoing genetic counseling, the couple was requested to terminate the pregnancy at 33 weeks and 2 days. The male fetus weighed 2,700 g and had a bifid nose. Upon external examination, all other parts were normal (Fig. 1G). Whole-exome sequencing (WES) analysis was executed using DNA extracted from the fetus's muscle tissue and the parents' blood. This study was approved by the Affiliated Women and Children's Hospital of Ningbo University Committee. Informed consent was obtained from the parents (approval number: EC2023-094).

Whole-exome sequencing

Genomic DNA (gDNA) was extracted from muscular tissue from the fetus and peripheral blood from the parents according to the manufacturer's instructions (Qiagen, Hilden, Germany). WES was conducted using the JunoXome OmniSeek *v*1 Kit (Twist Bioscience, San Francisco, CA, USA) and the MGISEQ-T7 platform (BGI, Shenzhen, China). Raw sequencing reads were aligned to the human reference genome, GRCh38/hg38, using Burrows-Wheeler Aligner(BWA). Single nucleotide variants (SNVs), insertions and deletions (INDELs) were called using the Genome Analysis Toolkit (GATK) HaplotypeCaller instrument and sentieon (2021.12). The identified variants were annotated using VEP (v105) and ANNOVAR (v2022.6.8) software. Notably, each variant was compared against public databases, including gnomAD (https://gnomad.broadinstitute.org/), the 1000 Genomes Project (https://www.internationalgenome.org/), and the Single-Nucleotide Polymorphism Database (dbSNP, https://www.ncbi.nlm.nih.gov/snp/). The effects of selected variants were predicted using SIFT, PolyPhen-2, Mutation Taster, SPliceAI, Human Splicing Finder (HSF), REVEL, and CADD. The classification of variants was performed based on the variant interpretation guidelines of American College of Medical Genetics and Genomics (ACMG) [9, 10].

Sanger sequencing

Potential causative variants were further validated using Sanger sequencing. The following primers were used: *FREM1*-F, 5′-TTGTTGTAGATGAGGGCTGCT-3′ and *FREM1*-R, 5′-ATTAAGCATGACCTGGCCAATCGCT-3′, based on the *FREM1* variant, c.3274 + 4 A > G. The polymerase chain reaction (PCR) products were purified using a TIANgel Midi Purification Kit (TianGen, Beijing, China). The products were analyzed using a 3500DX

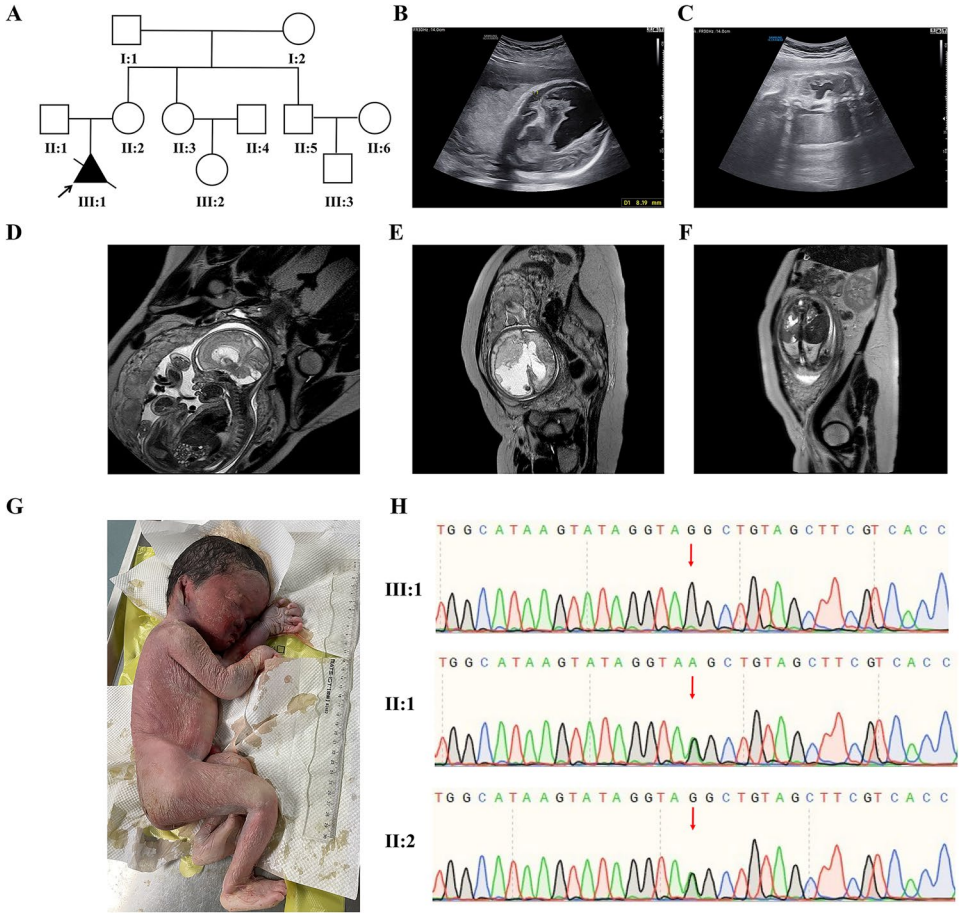

Fig. 1 Clinical features and sequence analysis of patients with *FREM1* variants. **A** Family pedigree. **B**-**C** Fetus ultrasound image at 32 weeks gestation shows that the left renal pelvis of the fetus was separated 12 mm, the upper ureter showed "beak-like changes", the posterior angle of the right lateral ventricle (LV) of the fetus reaches approximately 18 mm, the posterior angle of the left LV reaches approximately 32 mm, the third ventricle is dilated, and the widest part is 5.1 mm. A heterogeneous, slightly hyperechoic area measuring 67 × 28 mm was detected in the left cerebral parenchyma of the fetus, with partial cystic characteristics. **D**-**F** At 32^{+2} weeks of amenorrhea, the magnetic resonance image of the fetus shows a patchy area of a short T1 and prolonged T2 signal in the left LV near the fetal brain, with unclear boundaries and intrusion into the left LV. The left LV shows cistern-like and finger-like hydrops dilating and changing. The posterior horn is approximately 36 mm wide, while the posterior horn of the right LV is approximately 14.5 mm wide. The third ventricle shows cyst-like dilatation, with the midline structure slightly displaced to the right. The corpus callosum is visible. Short T1 signal shadows are observed on the lateral subdural and cerebral surfaces. The lower hemispheres of the cerebellum are clear, the vermis of the cerebellum is visible, and the hydrophilic expansion of the adjacent ventricles is visible. The subarachnoid space is widened in the posterior fossa. No obvious abnormality was found in the structure or signal of the cerebellar parenchyma. **G** The fetus following pregnancy termination at 33^{+2} weeks gestation shows a bifid nose. **H** Sanger sequencing revealed a homozygous splice variant, c.3274 + 4 A > G, of the *FREM1* gene in the proband. The mother and father were found to be heterozygous for this variant. The red arrow indicates the variant

Capillary Sequencer (Applied Biosystems, Foster City, CA, USA). The sequences were analyzed using Sequencing Analysis Software 6 (Applied Biosystems).

Construction and splicing analysis of the minigene

Wild-type (wt) *FREM1* was obtained by nested PCR using genomic DNA as the template. Deletion mutations were introduced using a pair of primers. Mutant (mut) *FREM1* was amplified using overlap extension PCR. The PCR products were digested with restriction enzymes before being ligated into the restriction sites of pcMINI (Bioeagle Biotech Company Ltd., Wuhan, China) and pcMINI-C to produce the recombinant plasmids pcMINI-*FREM1*-wt/mutant and pcMINI-C-*FREM1*-wt/mut. The recombinant plasmids were ligated overnight at 4 °C and then delivered to competent *Escherichia coli* DH5α cells. After 12 h, colony PCR was performed to verify the structures of the required base variations. To confirm this variation, the plasmids were sequenced. A Rapid Plasmid Mini Kit (Sigma Aldrich, St Louis, MO, USA) was used for plasmid extraction, according to the manufacturer's specifications. The recombinant plasmids were transiently transfected into HEK-293T and HeLa cells using Liposomal Transfection Reagent (SIMGEN, Hangzhou, China). Total RNA was extracted 2 days after

transfection using TRIzol reagent (TaKaRa, Dalian, China). cDNA was amplified using a reverse transcription kit (YESEN, Shanghai, China) according to the manufacturer's guidelines. The amplification products were subjected to 2% agarose gel electrophoresis and confirmed by Sanger sequencing. Table 1 lists the primer sequences used in the minigene assay.

In vivo reverse transcription splicing analysis

Total RNA was obtained from fetal muscular tissues and controls (muscle tissue from an induced abortion fetus at the same gestational age without pathogenic *FREM1* gene variants) using a MiniBEST Universal RNA Extraction Kit (TaKaRa, Dalian, China) according to the manufacturer's instructions. cDNA was reverse transcribed using a reverse transcription kit (TaKaRa, Dalian, China). The designed primers (*FREM1*-F1: 5′-CTCAGAGGCCGTGACATACA-3′, *FREM1*-R1: 5′-GGCTGGCTGCTTATTCTCAG-3′) were used for nested PCR with the reverse-transcribed cDNA as a template. The amplified products were subsequently subjected to further amplification using the primers *FREM*1-F2: 5′-CCCAATCCATCTGTTCCACT-3′ and *FREM1*-R2: 5′-AGCGCTGATGATGGAAGAGT C-3′). The PCR products were identified by electrophoresis on a 2% agarose gel and confirmed by Sanger sequencing.

Protein 3D structure analysis

The structure of human FREM1 was used as a template. The wt and mut FREM1 structures were predicted using AlphaFold3 [11]. The predicted tertiary structures were observed and aligned using the PyMol molecular visualization tool.

Table 1 Confirmation of the primers used for the minigene assay

Primer name	Sequences (5′-3′)
FREM1-MINI-BamHI-F	GCTCGGATCCttaaccttatttgcttttta
FREM1-MINI-XhoI-R	tttcCTCGAGcttttaaaccattctttctt
FREM1-mut-F	GCATAAGTATAGgtaggctgtagcttcgtca
FREM1-mut-R	tgacgaagctacagcctacCTATACTTATGC
FREM1-MINI-C-XhoI-R	AGACTCGAGAGTAATATTCTGCACTACAAA
FREM1-MINI-C-KpnI-F	ggtaGGTACCaattccataggtcaaagtaa
FREM1-61318-F2	gggacaaggacaacattgca
FREM1-61000-F1	ATACCCAGTAGACAACCAGC
FREM1-64320-R1	agaagccccgaccctaggca
FREM1-64148-R2	acatagccttccccactcc
FREM1-63389-R3	caaggtgctggattgagtgg
pcMINI-F	ACTTAAGCTTatgagtgggctttggggtggccggtt
pcMINI-R	GCCCTCTAGActggtcattccggctc
pcMINI-C-F	ACTTAAGCTTatgagtgggctttggggtggccggtt
pcMINI-C-R	TAGAAGGCACAGTCGAGG

Preimplantation genetic test for monogenic disorders (PGT-M) and prenatal genetic diagnosis

Whole-genome amplification (WGA) was performed on biopsied trophectoderm (TE) cells (approximately 5–8 cells) from each embryo using the multiple displacement amplification (MDA) method (REPLI-g Single Cell MDA kit, Qiagen, Germany) [12]. The whole-genome products were then purified using a DNA Clean-up Kit (CWBIO, Jiangsu, China). In addition to agarose electrophoresis, nanodrop quantification was used to determine the DNA quality. Each biopsy from the TE was added to MDA lysis buffer within PCR tubes for WGA and follow-up tests. In addition to Sanger sequencing, PCR amplification was performed to verify the *FREM1* c.3274 + 4 A > G variant in WGA and coupled products.

To avoid the misdiagnosis of allele dropout (ADO) and homologous reintegration of chromosomes, next-generation-sequencing-based haplotyping was performed using SNPs in the 2 Mb area flanking the target gene.

For TE specimens, low-depth whole-genome sequencing was performed for chromosome analysis. The DNA sequencing library was formulated without modifications, as previously described, using a gene sequencing library kit (Yikon Genomics, Shanghai, China). Libraries were sequenced on a MiSeq Dx platform using MiSeq Reagent Kit v3 (Illumina, San Diego, CA, USA). For CNV analysis, the FASTQ files were uploaded to the ChromGO platform. Within each embryo, duplications or deletions of more than 4 Mb were reported as calibrated reads. When the analysis was completed, the final results, such as quality control details and CNVs, were output.

Following the genetic diagnosis, embryo transfer was performed at our reproductive medical center. The selected embryo was delivered, resulting in an excellent pregnancy. Prenatal diagnosis was made through amniocentesis during the second trimester. Sanger sequencing, WES, karyotyping, and chromosomal microarray analysis (CMA) of amniotic fluid cells were used to validate the mutated *FREM1* allele and chromosomal normality.

Results

Genetic analysis

WES revealed that the proband harbored a homozygous variant, c.3274 + 4 A > G, in intron 18 of *FREM1* (NM_001379081.2). Sanger sequencing confirmed biparental inheritance (Fig. 1H). SpliceAI software predicted an acceptor loss score of 0.73, which reflects potential mRNA splicing. The variant has already been listed in gnomad v4.1.0, with an allele frequency of 0.00004539 in East Asia, and was previously described as a compound heterozygous variant with c.2078 + 1G > T in individuals with BNAR [8]. According to the ACMG criteria, the c.3274 + 4 A > G variant was initially categorized as

having uncertain significance (PM2_Supporting, PM3, and PP3).

Minigene splicing assay

To describe the influence of the variant at the mRNA level, we first implemented an in vitro minigene splicing assay. The minigene for pcMINI-*FREM1*-wt/mut was constructed by inserting part of intron 17 (391 bp), exon 18 (186 bp), and part of intron 18 (593 bp) into pcMINI (Fig. 2A). To determine whether the mutation affected the splicing of exon A-exon 18-exon B, pcMINI-*FREM1*-wt and pcMINI-*FREM1*-mut plasmids were transiently transfected into 293T and HeLa cells. Total RNA derived from cells transfected with pcMINI-*FREM1*-wt generated a 435 bp PCR product suggesting normal mRNA splicing. However, cells transfected with pcMINI-*FREM1*-mut generated a shorter product (255 bp; Fig. 2B). The mutant plasmid sequence showed that the c.3274 + 4 A > G mutation led to the complete deletion of exon 18, with cDNA and protein present as c.3089_3274del (p.Gly1030_Ile1091del) (Fig. 2C). Sequencing results validated the target segment of pcMINI-*FREM1*-wt/mut (Fig. 2D). The minigene for pcMINI-C-*FREM1*-wt/mut achieved consistent results (Fig. 3).

Moreover, we performed reverse transcription PCR (RT-PCR) splicing analysis in vivo. The WT sample possessed a single longer amplicon spanning approximately 528 bp, whereas the proband had a shorter amplicon (Fig. 4A). Sequencing analysis of the normal and short-sized bands confirmed the deletion of 62 amino acids in exon 18 of the shorter segment (Fig. 4C). Skipping exon 18 did not cause subsequent changes in the reading frame, but resulted in an internal loss of 62 amino acids,

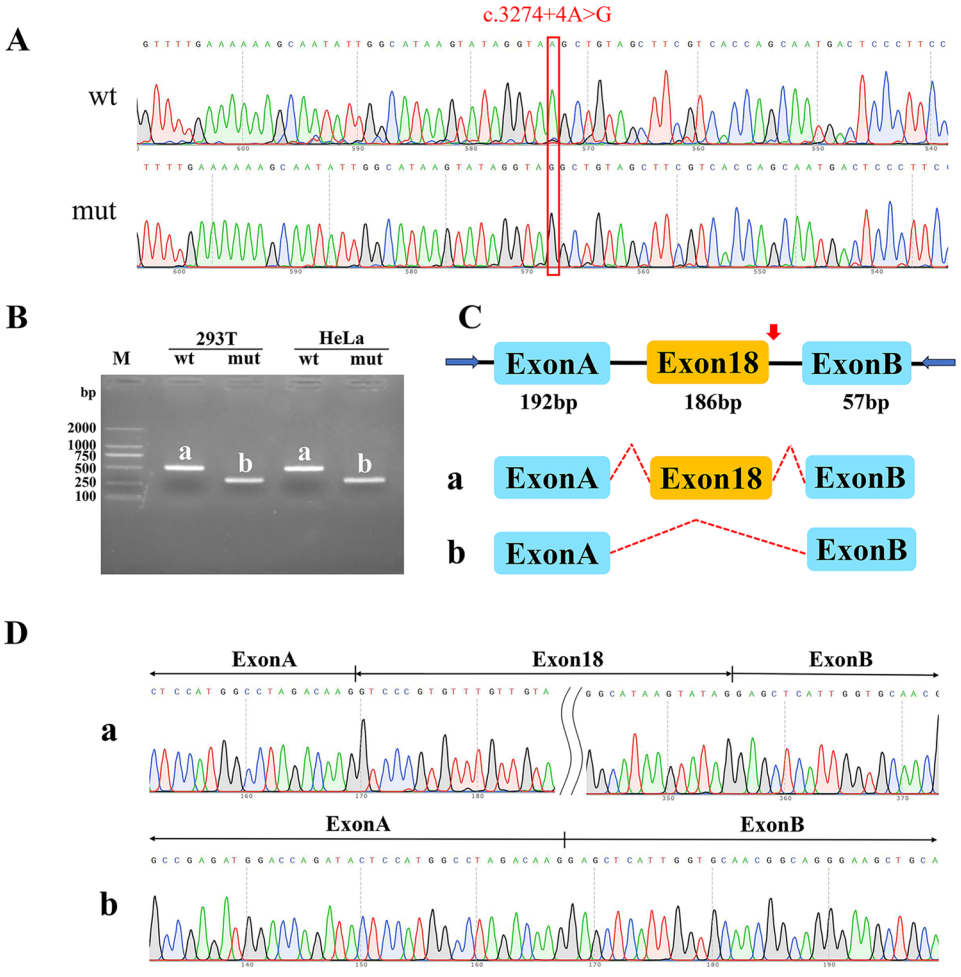

Fig. 2 Results of the pcMINI vector minigene assay. **A** Sequencing results showed that the target segment of the pcMIN-*FREM1*-wt/mut minigene was successfully introduced. **B** The pcMINI-*FREM1*-wt/wt plasmids were transfected into 293T and HeLa cells. Gel electrophoresis of the reverse transcription-polymerase chain reaction (RT-PCR) products show that the size of the wild-type product exceeded that of the mutant. **C** Illustration of the mini-gene construction and the c.3274 + 4 A > G variant–related abnormal splicing. The arrow indicates the location of the c.3274 + 4 A > G variant. **D** The minigene product sequencing outcomes were: **a** the wild-type minigene (pcMINI-*FREM1*-wt) formed a normal mRNA consisting of exon A, exon 18, and exon B and (**b**) the mutant mini-gene (pcMINI-*FREM1*-mut) triggered a splicing anomaly, triggering the deletion of exon 18

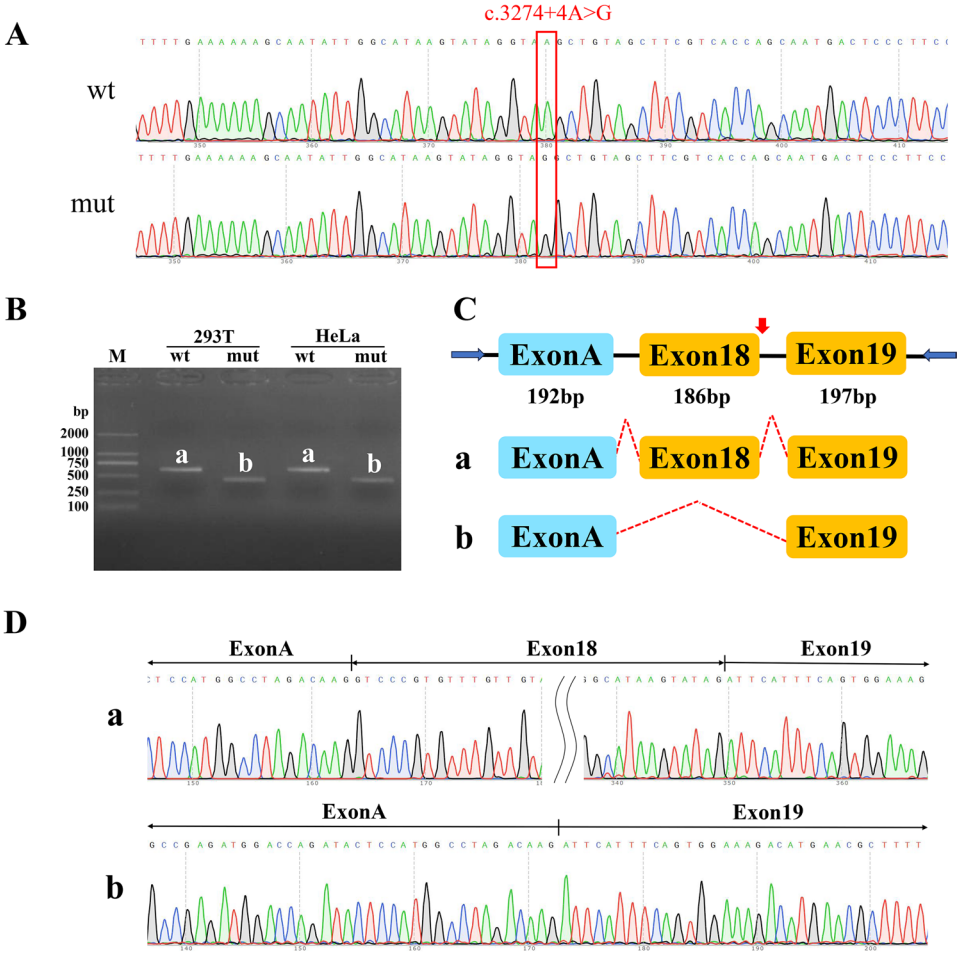

Fig. 3 Results of the pcMINI-C vector minigene assay. **A** Sequencing results showed that the target segment of the pcMIN-C-*FREM1*-wt/mut minigene was successfully introduced. **B** pcMINI-C-*FREM1*-wt/wt plasmids were transfected into 293T and HeLa cells. Gel electrophoresis of the RT-PCR products: the size of the wild-type band exceeded that of the mutant. **C** Schematic diagram of mini-gene construction and the c.3274 + 4 A > G variant–related abnormal splicing. The arrow indicates the location of the c.3274 + 4 A > G variant. **D** The minigene product sequencing results were: **a** the wild-type minigene (pcMINI-C-*FREM1*-wt) formed a normal mRNA consisting of exon A, exon 18, and exon 19; **b** the mutant mini-gene (pcMINI-C-*FREM1*-mut) triggered a splicing anomaly, triggering the exon 18 deletion

which may have produced a truncated protein with a length of 2,117 amino acids (Fig. 4B).

Structural analysis of the identified *FREM1* variant

We evaluated the effects of *FREM1* variants on this protein using in silico methods. The FREM1 protein contains 12 chondroitin sulfate proteoglycan (CSPG) domains that function in concert to endow the protein with the function of a cell surface receptor. Under normal circumstances, the CSPG domains form a sheet-like structure interwoven by multiple β-sheets (as shown in the orange part of Fig. 5A). However, due to the deletion of 62 amino acids, the CSPG6 domain in the variant is severely disrupted, retaining only a single β-sheet and presenting an aberrant α-helix (Fig. 5B). In view of these outcomes, the function of the protein encoded by the *FREM1* gene is changed. Therefore, we speculated that this variant might weaken the signal transduction ability of the protein and impair FRAS1/FREM complex interaction. Combined with the functional experimental results, evidence for the c.3274 + 4 A > G variant was upgraded to a likely pathogenic variant (PVS1_Moderate, PM2_Supporting, PM3, and PP4). The fetus was diagnosed with BNAR based on the clinical phenotype and molecular genetic manifestations.

PGT-M and prenatal diagnosis

The couple experienced a single pre-implantation genetic test (PGT) cycle, in which four embryos (E1-4) ultimately developed into blastocysts after intracytoplasmic sperm injection. Following TE biopsy, 5–8 cells were used for whole-genome amplification. No CNVs exceeding 4 Mb or aneuploidies were found in E1 or E3. E2 was considered a mosaic embryo (Fig. 6A). Linkage analysis based on pedigree SNP haplotypes showed that E1 inherited pathogenic variants, and was not recommended for

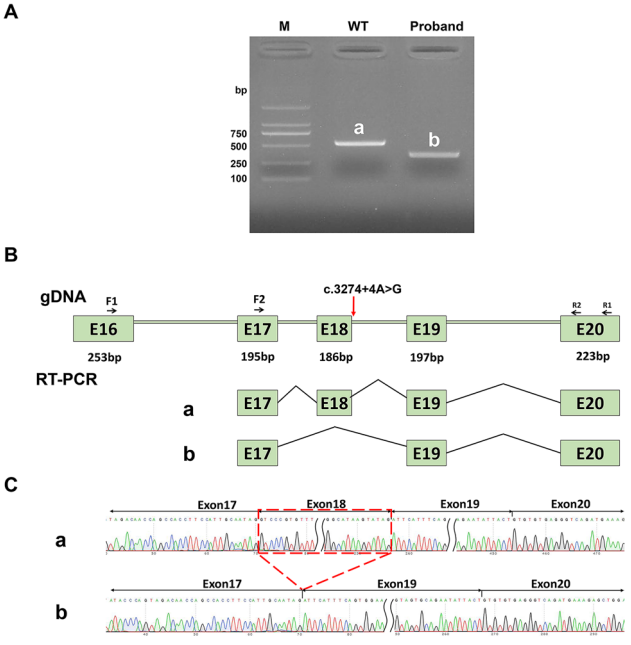

Fig. 4 Results of the minigene splicing assay in vivo. **A** Agarose gel electrophoresis of RT-PCR products. The wild-type band is labeled "a", and the proband bands are labeled "b". A longer amplicon of approximately 528 bp observed in controls aligned with the anticipated band size. The b-band (342 bp) is shorter than the a-band. **B** Schematic diagram of primer design and the c.3274 + 4 A > G–variant related aberrant splicing. The red arrow denotes the variant position. **C** Sequencing analysis of splicing bands **a** and **b**. Band a indicates for normal splicing, with the splicing mode as exon 17 (195 bp)-exon 18 (186 bp)-exon 19 (197 bp)-exon 20 (223 bp); band b indicates aberrant splicing showing exon 18 skipping, with the splicing mode as exon 17 (195 bp)-exon 19 (197 bp)-exon 20 (223 bp)

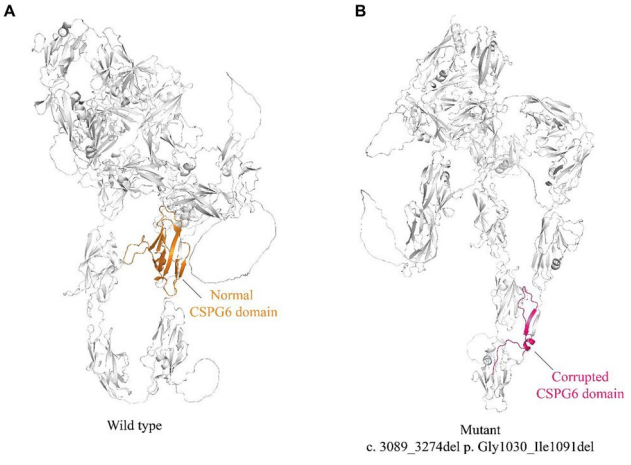

Fig. 5 The predicted three-dimensional structure of FREM1. **A** The structure depicts wild type FREM1 (orange denotes the CSPG6 domain). **B** The amino acid sequence deletion as a result of the c.3089_3274del variant is underscored in pink. The structure specifically highlights the corrupted CSPG6 domain (only one beta fold was retained and an abnormal alpha helix appeared) of FREM1

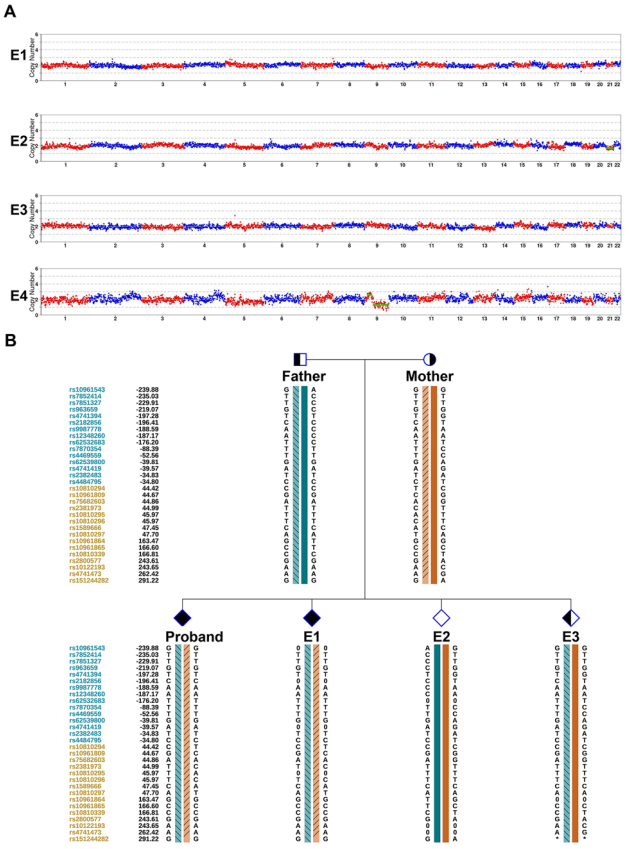

Fig. 6 Prenatal genetic test for monogenic disorders of the embryos. **A** Copy number variation (CNV) outcomes of the embryos. E1 and E3 are euploid embryos. E2 exhibits mosaic monosomy of chromosome 21. E4 shows a 20 Mb mosaic duplication of chromosome 9p23p21.1 and a 102.8 Mb deletion on chromosome 9, spanning from p13.1 to q34.3. **B** Results of haplotype linkage analysis. The haplotype linkage analysis is illustrated for family members and embryos. The left side displays the reference SNP cluster ID numbers. The dark blue and orange ID numbers indicate downstream and upstream informative SNPs, respectively. The dark blue and dark orange bars signify the normal haplotypes of the mothers and fathers, respectively. The blue bars full of slashes show the paternal mutational haplotype, with the orange bars full of slashes signifying the maternal mutational haplotype. E1 is the patient, E2 is a normal embryo, and E3 is a paternal mutational carrier

transfer. E2 did not inherit pathogenic variants. E3 inherited only the paternal risk allele and was classified as a carrier embryo. E4 amplification failed (Fig. 6B). Sanger sequencing of the four embryos yielded results concordant with the haplotype analysis, with the exception of an ADO event in E3. Additionally, E4 exhibited segmental deletions and duplications, alongside mosaic signals across multiple chromosomes (Table 2).

Despite the ADO event, haplotype analysis definitively confirmed embryo E3 as a heterozygous carrier of the pathogenic variant. Given the autosomal recessive inheritance pattern of BNAR syndrome, this carrier embryo is clinically unaffected and suitable for transfer. Exhibiting appropriate developmental progression and

Table 2 Summary of the detection results of the four biopsied blastocysts

Embryo ID	Biopsy date	Gardner grade	CNV analysis	SNP haplotype	Sanger Sequencing
E1	D5	4BB	46, XN	Patient	c.804 + 2 T > C, homozygote
E2	D5	4BB	46, XN, -21(×1, mos, ~ 32%)	Normal	Normal
E3	D5	4BB	46, XN	Paternal carrier	ADO
E4	D5	4BB	46, XN, dup(9)(p23p21.1) (~ 20.00 Mb,~60%),del(9)(p13.1q34.3) (~ 102.80 Mb)	Amplification failure	Amplification failure

CNV copy number variant (detected using low-pass whole-genome sequencing), *SNP* single-nucleotide polymorphism (detected using multiplex polymerase chain reaction and targeted next-generation sequencing)

morphological quality (Day 5 blastocyst, grade 4BB), E3 was selected for implantation. Following comprehensive genetic counseling, the patient underwent a single embryo transfer, resulting in a successful clinical pregnancy. A prenatal test using amniocentesis was performed at 19^{+3} weeks of age. WES and Sanger sequencing showed heterozygous variations in *FREM1* c.3274 + 4 A > G, but no chromosomal anomalies were detected by karyotyping or CMA. Throughout the pregnancy, total ultrasonographic examination showed no morphological fetal anomalies. The patient delivered a full-term girl at full term at the Affiliated Women and Children's Hospital of Ningbo University. No anomalies were observed during the examination of the newborn. Until now, follow-up assessments at 6 months of age have illustrated outstanding outcomes.

Discussion

FREM1 autosomal recessive diseases encompass BNAR syndrome, Manitoba oculotrichoanal (MOTA) syndrome, and isolated congenital anomalies of the kidney and urinary tract (CAKUT) [1, 8, 13, 14]. MOTA is a rare disorder characterized by cryptophthalmos; eyelid colobomas; microphthalmia/anophthalmia; an abnormal hairline; a broad or bifid nasal tip; and gastrointestinal abnormalities, such as anal stenosis and omphalocele [13, 15]. For example, Slavotinek et al. [15] reported that eye defects occur in patients with MOTA syndrome, yet they have not been reported in patients with BNAR. Conversely, renal agenesis is a characteristic of BNAR, but has not been detected in MOTA syndrome. *FREM1*-CAKUT has been identified in individuals with renal hypodysplasia and vesicoureteral reflux [14]. However, the incidences of these syndromes have not been established [16]. Symptoms may vary in severity, even within the same family. Usually, growth and psychomotor development are normal. Since the discovery of BNAR in 2002, 14 patients have been reported, including our patient [1, 2, 7, 8]. Most cases present with a bifid nose (93.33%, 15/14); a short, thick oral frenula (66.67%, 4/6); renal malformations (64.29%, 9/14); anorectal malformations (25%, 3/12); limb anomalies (25%, 3/12); airway malformations (16.67%, 2/12); and delayed developmental milestones (10%, 1/10). A bifid nose is the most commonly reported symptom (Table 3).

The human *FREM1* gene is located on chromosome 9p22.3 and contains 46 exons. FREM1 is expressed in areas of epidermal-mesenchymal interplay and exhibits significant embryonic expression. The developing nose is largely located in the epithelial-mesenchymal transitional region at the two medial nasal processes [17, 18]. The FREM1 protein contains a putative signal sequence, 12 CSPG repeats, a calx-β region, and a C-terminal type C lectin-like region [2, 19]. Previously published causative variants have been positioned throughout the CSPG domains [7], and the c.3274 + 4 A > G variant identified in our case was located in the sixth CSPG repeat. Pathogenic variants of *FREM1* may disrupt CSPG domains and impair the interplay between proteins of the FRAS1/FREM complex [4, 20, 21]. FREM1 plays a critical role in craniofacial and renal development. Analysis of the mouse craniofacial skeleton demonstrated that homozygous *Frem1*^{bat} mice exhibit a significantly shorter upper midface, encompassing the nasal bone and premaxilla, as well as slightly wider nasal bones, with heterozygous mice displaying similar but less pronounced phenotypic alterations [2, 5]. In addition, *FREM1* is sufficient to induce cranial neural crest cell growth in a concentration-dependent manner, and Sonic Hedgehog signaling pathway antagonism decreases Frem1 expression levels in the etiology of midfacial hypoplasia [18]. These observations concur with the early expression of Frem1 in developing facial prominences and the function of recessive *FREM1* variants in BNAR syndrome.

In this study, we describe a Chinese patient affected by hydrocephalus, cerebral hemorrhage, left hydronephrosis, and dysmorphic features harboring a newly described homozygous variant in the *FREM1* gene:

Table 3 BNAR-related clinical manifestations and literature review

References	This study	[1]	[2]	[7]	[8]
No. of patients	1	4	5	2	1
Origin	China	Egypt	Afghanistan; Pakistani	Turkey	Germany
Consanguinity	Non-consanguineous	Consanguineous	Consanguineous	Consanguineous	NA
Gender	Female	2 female, 2 male	UK	1 female, 1 male	NA
Age range at last assessment	At 32 weeks of gestation	At birth	UK	12 years,22 years	NA
Fetus during pregnancy	Intracranial hemorrhage, hydrocephalus, left hydronephrosis, upper ureter obstruction	3 normal, 1 severe Oligo-hydramnios, prenatal ultrasound revealed bilateral renal agenesis	UK	1unilateral renal agenesis and congenital heart disease, 1 normal	Urogenital sinus hydronephrosis, unilateral renal agenesi, hydrometrocolpos, cloacal malformation
Bifid nose	1/1	4/4	5/5	2/2	0/1
Anorectal malformation	0/1	3/4	0/5	0/2	UK
Airway malformation	0/1	0/4	0/5	2/2	UK
Renal agenesis	1/1	4/4	2/5	1/2	1/1
Short, thick oral frenula	UK	3/4	NA	1/2	UK
Limb anomalies	0/1	3/4	0/5	2/2	UK
Developmental milestones	UK	0/3	0/5	1/2	UK
Variant	c.3274 + 4 A > G	c.2721delG(p.V908SfsX17)	c.1945 C > T (p.R649W); c.4318G > A (p.G1440S)	E19-30del	c.2078 + 1G > T(p.?)/ c.3274 + 4 A > G(p.?)
Genotypes	Homozygotes	Homozygotes	Homozygotes	Homozygotes	Compound heterozygote
Variant consequences	Splicing	Frameshifts	Missense	Microdeletion	Splicing

UK unknown

c.3274 + 4 A > G. SpliceAI, RT-PCR, and minigene array analyses were performed to explore the etiology of the splicing variation. The variant led to a 63 bp deletion and skipping of exon 18. Using AlphaFold predictions, an approximate model of the overall structure was obtained. It largely consisted of 12 β-strands. Specifically, the c.3274 + 4 A > G variant disrupts the CSPG6 domain, providing robust evidence that it is an in-frame deletion that alters the protein length and contributes to the pathogenesis of BNAR. Notably, Koenigbauer et al. reported a case involving a complex variant of c.3274 + 4 A > G and c.2078 + 1G > T that exhibited hydronephrosis, cloacal malformation, urogenital sinuses, hydrometrocolpos, and unilateral renal agenesis [8]. Yang et al. [22] oobserved that pathogenic variants of *FREM1* were related to acute prenatal hydrocephalus and shortened limbs in prenatal patients. However, the prenatal phenotypes of cerebral hemorrhage detected by ultrasound in our patient did not overlap with those of BNAR or MOTA cases, as reported in previous cases of homozygous or compound heterozygous variants of the *FREM1* gene. Overall, the pathogenicity of the c.3274 + 4 A > G variant has been reclassified as likely pathogenic. Herein, we report a fetal case homozygous for this variant, expanding the phenotypic spectrum of BNAR syndrome to include a novel manifestation of intracranial hemorrhage. While *FREM1* mutations are classically associated with epithelial and craniofacial anomalies, the observed intracranial hemorrhage suggests an underrecognized role in vascular integrity. We hypothesize two potential mechanisms for this novel central nervous system phenotype. First, given the essential function of the FREM1 protein in anchoring basement membranes via the FRAS1/FREM complex, its disruption may directly compromise the structural stability of the cerebrovascular endothelium, predisposing developing blood vessels to spontaneous rupture [3]. Second, alternative splicing of FREM1 produces the TILRR isoform, a co-receptor critical for interleukin-1 signaling [23]. Pathogenic variants disrupting this pathway could induce localized neuroinflammation or endothelial dysfunction, further exacerbating vascular fragility. Future functional studies examining neurovascular basement membrane. To date, only Six *FREM1* variants have been associated with BNAR, and the genotype-phenotype correlation remains unclear (Table 3). Following the proband's diagnosis of BNAR, the couple selected PGT-M and prenatal diagnosis

to prevent the delivery of specific variants to their offspring.

Our study has some limitations, such as missing information about detailed postmortem investigations and developmental assessments. This issue must be addressed in future studies. Our findings confirm the demand for a molecular genetic diagnosis of BNAR. Minigene assays contribute to the characterization of cases of abnormal splicing due to candidate splicing variants. Trio-WES is a valid high-throughput method for diagnosing BNAR and other ultrasonic structural abnormalities.

Conclusions

We report that a homozygous variant of the *FREM1* gene, c.3274 + 4 A > G in a Chinese fetus with BNAR. This variant affects normal mRNA splicing, which may contribute to the progression of fetal BNAR. Follow-up functional research is required to provide in-depth evidence based on the assumption that the c.3274 + 4 A > G variant may disrupt the maintenance of normal FREM1 protein function and stability, leading to BNAR.

Abbreviations

BNAR	Bifid nose with or without anorectal and renal anomalies
ECM	Extracellular matrix
MRI	Magnetic resonance imaging
WES	Whole-exome sequencing
gDNA	Genomic DNA
SNVs	Single nucleotide variants
INDELs	Insertions and deletions
GATK	Genome Analysis Toolkit
HSF	Human Splicing Finder
ACMG	American College of Medical Genetics and Genomics
PCR	Polymerase chain reaction
PGT-M	Preimplantation genetic test for monogenic disorders
WGA	Whole-genome amplification
TE	Trophectoderm
MDA	Multiple displacement amplification
ADO	Allele dropout
CMA	Chromosomal microarray analysis
CSPG	Chondroitin sulfate proteoglycan
MOTA	Manitoba oculotrichoanal
CAKUT	Congenital anomalies of the kidney and urinary tract

Acknowledgements

We are grateful to the patients and the family members who participated in this study.

Authors' contributions

LLY performed the material preparation, data collection, analysis and wrote the first draft of the manuscript. YWL coordinated the study and helped draft review. YXZ and CXH collected the clinical data, and analysis. JC and HJL data collection, and genetic counseling. JHZ performed bioinformatics and statistical analyses. HBL contributed to the study conception, design, and wrote the final draft of the manuscript. All authors have read the approved final manuscript.

Funding

This research was funded by the Affiliated Women and Children's Hospital of Ningbo University, Ningbo science and technology project (Grant No. 2023Z178), Natural Science Foundation of Ningbo Municipality (Grant No. 2024J358), Innovation Project of Distinguished Medical Team in Ningbo (Grant No. 2022020405), Key Technology Breakthrough Program of Ningbo Sci-Tech Innovation YONGJIANG 2035 (Grant No. 2024Z221).

Data availability

All data generated or analysed during this study are included in the article. The variant reported in this article were deposited into ClinVar with accession numbers: SCV005908103.

Declarations

Ethics approval and consent to participate

Ethics approval was from the Affiliated Women and Children's Hospital of Ningbo University, and written informed consents were signed by the patients before this study.

Consent for publication

Not applicable.

Competing interests

The authors declare no competing interests.

Author details

[1]The Central Laboratory of Birth Defects Prevention and Control, The Affiliated Women and Children's Hospital of Ningbo University, Ningbo, Zhejiang 315000, China
[2]Ningbo Key Laboratory for the Prevention and Treatment of Embryogenic Diseases, The Affiliated Women and Children's Hospital of Ningbo University, Ningbo, Zhejiang 315000, China
[3]Ningbo Key Laboratory of Genomic Medicine and Birth Defects Prevention, The Affiliated Women and Children's Hospital of Ningbo University, Ningbo, Zhejiang 315000, China
[4]Department of Obstetrics, The Affiliated Women and Children's Hospital of Ningbo University, Ningbo, Zhejiang 315000, China
[5]Department of Obstetrics, The Affiliated Lihuili Hospital of Ningbo University, Ningbo, Zhejiang 315000, China

Received: 12 January 2026 / Accepted: 27 March 2026
Published online: 02 April 2026

References

1. Al-Gazali LI, Bakir M, Hamud OA, Gerami S. An autosomal recessive syndrome of nasal anomalies associated with renal and anorectal malformations. Clin Dysmorphol. 2002;11(1):33–8.
2. Alazami AM, Shaheen R, Alzahrani F, Snape K, Saggar A, Brinkmann B, et al. FREM1 mutations cause bifid nose, renal agenesis, and anorectal malformations syndrome. Am J Hum Genet. 2009;85(3):414–8.
3. Pavlakis E, Chiotaki R, Chalepakis G. The role of Fras1/Frem proteins in the structure and function of basement membrane. Int J Biochem Cell Biol. 2011;43(4):487–95.
4. Kiyozumi D, Sugimoto N, Sekiguchi K. Breakdown of the reciprocal stabilization of QBRICK/Frem1, Fras1, and Frem2 at the basement membrane provokes Fraser syndrome-like defects. Proc Natl Acad Sci U S A. 2006;103(32):11981–6.
5. Vissers LE, Cox TC, Maga AM, Short KM, Wiradjaja F, Janssen IM, et al. Heterozygous mutations of FREM1 are associated with an increased risk of isolated metopic craniosynostosis in humans and mice. Plos Genet. 2011;7(9):e1002278.
6. Chacon-Camacho OF, Zenker M, Schanze D, Ledesma-Gil J, Zenteno JC. Novel FREM1 mutations in a patient with MOTA syndrome: Clinical findings, mutation update and review of FREM1-related disorders literature. Eur J Med Genet. 2017;60(3):190–4.
7. Brischoux-Boucher E, Dahlen E, Gronier C, Nobili F, Marcoux E, Alkuraya FS, et al. Bifid nose as the sole manifestation of BNAR syndrome, a FREM1-related condition. Clin Genet. 2020;98(5):515–6.
8. Koenigbauer JT, Fangmann L, Reinhardt C, Weichert A, Henrich W, Saskia B, Gabriel HP. Spectrum of congenital anomalies of the kidney and urinary tract (CAKUT) including renal parenchymal malformations during fetal life and the implementation of prenatal exome sequencing (WES). Arch Gynecol Obstet. 2024;309(6):2613–22.

9. Nykamp K, Anderson M, Powers M, Garcia J, Herrera B, Ho YY, et al. Sherloc: a comprehensive refinement of the ACMG-AMP variant classification criteria. Genet Med. 2017;19(10):1105–17.
10. Richards S, Aziz N, Bale S, Bick D, Das S, Gastier-Foster J, et al. Standards and guidelines for the interpretation of sequence variants: a joint consensus recommendation of the American College of Medical Genetics and Genomics and the Association for Molecular Pathology. Genet Med. 2015;17(5):405–24.
11. Abramson J, Adler J, Dunger J, Evans R, Green T, Pritzel A, et al. Accurate structure prediction of biomolecular interactions with AlphaFold 3. Nature. 2024;630(8016):493–500.
12. Dean FB, Hosono S, Fang L, Wu X, Faruqi AF, Bray-Ward P, et al. Comprehensive human genome amplification using multiple displacement amplification. Proc Natl Acad Sci U S A. 2002;99(8):5261–6.
13. Li C, Marles SL, Greenberg CR, Chodirker BN, van de Kamp J, Slavotinek A, et al. Manitoba Oculotrichoanal (MOTA) syndrome: report of eight new cases. Am J Med Genet A. 2007;143A(8):853–7.
14. Kohl S, Hwang DY, Dworschak GC, Hilger AC, Saisawat P, Vivante A, et al. Mild recessive mutations in six Fraser syndrome-related genes cause isolated congenital anomalies of the kidney and urinary tract. J Am Soc Nephrol. 2014;25(9):1917–22.
15. Slavotinek AM, Baranzini SE, Schanze D, Labelle-Dumais C, Short KM, Chao R, et al. Manitoba-oculo-tricho-anal (MOTA) syndrome is caused by mutations in FREM1. J Med Genet. 2011;48(6):375–82.
16. Berrada S, Tazzite A, Bouzroud W, Gazzaz B, Lehlimi M, Dehbi H. Novel FREM1 homozygous variant in an individual with an intermediate phenotype between Bifid Nose with or without Anorectal and Renal Anomalies and Manitoba-oculo-tricho-anal syndromes. Clin Dysmorphol. 2023;32(1):36–8.
17. Petrou P, Chiotaki R, Dalezios Y, Chalepakis G. Overlapping and divergent localization of Frem1 and Fras1 and its functional implications during mouse embryonic development. Exp Cell Res. 2007;313(5):910–20.
18. McLaughlin MT, Sun MR, Beames TG, Steward AC, Theisen J, Chung HM, et al. Frem1 activity is regulated by Sonic hedgehog signaling in the cranial neural crest mesenchyme during midfacial morphogenesis. Dev Dyn. 2023;252(4):483–94.
19. Staub E, Hinzmann B, Rosenthal A. A novel repeat in the melanoma-associated chondroitin sulfate proteoglycan defines a new protein family. Febs Lett. 2002;527(1–3):114–8.
20. Wiradjaja F, Cottle DL, Jones L, Smyth I. Regulation of PDGFC signalling and extracellular matrix composition by FREM1 in mice. Dis Model Mech. 2013;6(6):1426–33.
21. Kiyozumi D, Sugimoto N, Nakano I, Sekiguchi K. Frem3, a member of the 12 CSPG repeats-containing extracellular matrix protein family, is a basement membrane protein with tissue distribution patterns distinct from those of Fras1, Frem2, and QBRICK/Frem1. Matrix Biol. 2007;26(6):456–62.
22. Yang YD, Huang LY, Yan JM, Han J, Zhang Y, Li DZ. Novel FREM1 mutations are associated with severe hydrocephalus and shortened limbs in a prenatal case. Eur J Obstet Gynecol Reprod Biol. 2017;215:262–4.
23. Smith SA, Samokhin AO, Alfadi M, Murphy EC, Rhodes D, Holcombe WML, et al. The IL-1RI Co-Receptor TILRR (FREM1?Isoform 2) Controls Aberrant Inflammatory Responses and Development of Vascular Disease. JACC Basic translational Sci. 2017;2(4):398–414.

Publisher's Note